The mechanism of oxygen catalytic reduction in the presence of platinum and silver nanoparticles

N. A. Yashtulov,[a]* A. A. Revina,[b] and V. R. Flid[a]

[a]M. V. Lomonosov Moscow State Academy of Fine Chemical Technology,
86 Vernadskogo prosp., 119571 Moscow, Russian Federation.
Fax: +7 (495) 434 7111. E-mail: YashtulovNA@rambler.ru
[b]A. N. Frumkin Institute of Physical Chemistry and Electrochemistry, Russian Academy of Sciences,
31 Leninsky prosp., 119991 Moscow, Russian Federation
Fax: +7 (495) 955 4017

The reaction of oxygen reduction on the mercury electrode in the solution of the reversed micelles and in the presence of platinum and silver nanoparticles was studied. The data of inverse voltammetry show that in the presence of platinum nanoparticles the reaction can proceed *via* both two-electron and four-electron reaction mechanisms. In the case of silver nanoparticles it proceeds in accordance with the two-electron mechanism. Cumulative effect of catalytic action of platinum and silver nanoparticles on the molecular oxygen reduction was found.

Key words: oxygen reduction, platinum and silver nanoparticles, catalytic mechanism.

The reaction of oxygen reduction (OR) is one of the most important multistage processes in the kinetics and catalysis. It is of the great theoretical and practical value. The studies of OR mechanisms in the electrochemical energy generators (ECEG) are the most topical. In the ECEG the molecular oxygen or some oxygen-containing substances are used as the oxidants of different kinds of fuel. Nanomaterials such as carbon nanotubes, carbon fibers, fulleroids, porous silicon, polymer composites, and nanocatalysts received increasing application in these generators.

In the series of our works[1—4] and in the other publications[5—8] the efficiency of nanoparticles of silver and of platinum group metals as electrocatalyst of OR on the porous supports such as porous silicon and carbon nanotubes was shown. Such nanocatalysts are produced by the radiation chemical synthesis in the reversed micelles of the stable metal nanoparticles.[9,10] By using this method the nanosized metal particles can be prepared. When incorporated into solid nanocomposites they retain activity for a long period of time upon the contact with the liquid phase.

Platinum and the platinum-based composites are considered as the best catalysts for the OR in ECEG. The cost of the catalysts can be considerably reduced due to the introduction of nanostructured catalyst such as platinum nanoparticles on the surface of stabilizing support. As OR proceeds at high values of cathode potential the oxygen reduction is accompanied by the formation of side products such as peroxides and radicals capable to decrease catalyst activity. To suppress the peroxide action on platinum, the silver additives promoting the peroxides decomposition are usually used.

The overall process of OR is described by following equations:[9—12]

$$O_2 + 4\,H^+ + 4\,e^- \xrightarrow{i} 2\,H_2O,$$

$$O_2 + 2\,H_2O + 4\,e^- \xrightarrow{ii} 4\,OH^-.$$

i. Acidic medium; *ii*. Basic medium.

Two mechanisms of the overall process are possible. The first mechanism is the four-electron route and it proceeds with the direct cleavage of the double bond in the oxygen molecule dissociatively adsorbed on the surface at the first process step which is the rate-limiting one:

$$O_2 \longrightarrow 2\,O_{ads}. \qquad (1)$$

Then follows the second, a more rapid step:

$$2\,O_{ads} + 4\,H^+ + 4\,e^- \longrightarrow 2\,H_2O. \qquad (2)$$

The second mechanism of OR is the two-electron route and it consists of two two-electron steps and accompanied with the formation of peroxides. The first step is described by the equation:

$$O_2 + 2\,H^+ + 2\,e^- \longrightarrow H_2O_2. \qquad (3)$$

Published in Russian in *Izvestiya Akademii Nauk. Seriya Khimicheskaya,* No. 8, pp. 1456—1461, August, 2010.

This step consists of two sub-steps: first sub-step (3a) is the rate-limiting one, the second sub-step (3b) results in formation of peroxides.

$$O_2 + H^+ + e^- \longrightarrow HO_2^{\cdot}$$

$$(O_2 + e^- \longrightarrow O_2^-,\ O_2^- + H^+ \longrightarrow HO_2^{\cdot}). \tag{3a}$$

$$HO_2^{\cdot} + H^+ + e^- \longrightarrow H_2O_2$$

$$(HO_2^{\cdot} + e^- \longrightarrow HO_2^-,\ HO_2^- + H^+ \longrightarrow H_2O_2^{\cdot}). \tag{3b}$$

The second step (4) which also involves two sub-steps (4a), (4b), is the step of the product formation (H_2O) during the reduction of hydrogen peroxide:

$$H_2O_2 + 2\,H^+ + 2\,e^- \longrightarrow 2\,H_2O, \tag{4}$$

$$H_2O_2 + e^- \longrightarrow HO^{\cdot} + HO^-, \tag{4a}$$

$$HO^{\cdot} + HO^- + e^- + 2\,H^+ \longrightarrow 2\,H_2O. \tag{4b}$$

During the reduction of molecular oxygen on the platinum group metals and on the silver the only one wave, corresponding to the four-electron mechanism (reactions (1), (2)) is detected on voltammetric curves. On the mercury and carbon electrodes only two-electron mechanism with the step of intermediate H_2O_2 formation is possible. Two broad waves corresponding to two steps (formation of H_2O_2 (reaction (3)) and reduction of H_2O_2 to the product H_2O (reaction (4)) are observed on voltammeric curves. The limiting reaction of the overall two-electron mechanism is the addition of the first electron to the oxygen molecule according to the first sub-step of the first stage (reaction (3a)). On the step of H_2O_2 reduction to H_2O (reaction (4)) the rate of the first sub-step (reaction (4a)) is considerably lower than the rate of the second (reaction (4b))[9]. The rate decrease at any step causes the polarization (the process of the change of the potential of electrode reaction with respect to the equilibrium value). The reason of polarization is determined by the nature of limiting step. The value of the potential shift is considered as the overcurrent.

The aim of the present study is the refinement of the mechanism of catalytic action of Pt and Ag nanoparticles in OR on dropping mercury electrode (DME) in the solutions of reversed micelles by the method of alternating-current inverse voltammetry (ACIV).

Experimental

The ACIV measurements were conducted on a ABC 1.1 voltammetry polarograph with the build-in Modul EM-04 sensor (Certificate of Russian Federation No. 7936), providing the square-wave modulation of a potential sweep. The working electrode was DME, the secondary electrode was platinum, the reference electrode was the saturated silver-chloride Ag/AgCl/KCl (E = +0.20 V) electrode. The polarograph allows one to achieve the sensitivity of analysis up to 10^{-8} mol L^{-1} at the background/substance ratio up to 10^{-4}, what makes it possible to analyse any of redox pairs independent of their extent of reversibility. The device operation mode was one with alternating current, the potential sweep interval was up to 1600 mV, and the sweep rate was from 1 to 200 mV s^{-1} with a 1 mV step.

The mercury electrode is the one with a high degree of polarization. The interval of potentials of DME applications for the electro-analytical purposes is substantially extended from the cathode region, which is typical of OR. Therefore DME is suitable for the study of OR mechanisms without competitive influence of the other reactions.

The platinum and silver nanoparticles were synthesized according to the procedure described earlier.[13,14] The reversed micelles are microdrops of aqueous solution (pools stabilized with surfactant in the organic solvent — isooctane). The metal nanoparticles form in the pool of micelle at radiofrequency ^{60}Co γ-irradiation. By varying conditions of synthesis as well as reagent concentrations it is possible to control the size range of the particles formed. For the reversed micelles preparation 0.15 M solution of surfactant (sodium bis(2-ethylhexyl)sulfosuccinate (SES) 99%, Sigma) in isooctane was used. The molar ratio water : surfactant was varied from 1.5 to 5, that corresponds to solubilization extent $\omega_0 = [H_2O]/[SES] = 1.5—5$.

The intervals of Pt nanoparticles concentration in the solutions of reversed micelles dependent on ω_0 are listed below.

ω_0	C(Pt)/mol L^{-1}
1.5	$1.40 \cdot 10^{-5}—1.12 \cdot 10^{-4}$
3.0	$2.80 \cdot 10^{-5}—2.80 \cdot 10^{-4}$
5.0	$4.66 \cdot 10^{-5}—3.26 \cdot 10^{-4}$

For the Ag nanoparticles at ω_0 = 1.5 the concentration increased from $1.2 \cdot 10^{-4}$ to $1.2 \cdot 10^{-3}$ mol L^{-1}.

According to foton-correlation, HPLC and high-resolution scanning electron microscopy data[2—4] the size range for the synthesized nanoparticles is within 2—14 nm, whereas for Ag nanoparticles it is within 4.5—11 nm. When the solubilization extent ω_0 increases the share of fraction with the larger sizes also increases.

The water-ethanol (1 : 1) solution of phosphate buffer with pH 6.86 was used as a background solution. The molecular oxygen concentration was maintained constant in the water-ethanol solution ($8.5—9 \cdot 10^{-4}$ mol L^{-1}) by bubbling the air through the system before the each measurement. Such value corresponds to the oxygen solubility in the solution. Voltammetry curves were registered in a 20 mL electrochemical cell. Each measurement was performed on the renewed surface of the mercury drop. The same background solution was applied during the measurements.

Results and Discussion

The values of potentials (E) the peak maxima of OR on DME with respect to saturated silver-chloride electrode Ag|AgCl|KCl and corresponding to them currents (I^-), read from the baseline are listed in Table 1 as a function of the Pt nanoparticles concentrations at the solubilization extent ω_0 = 1.5.

Table 1. The influence of concentration of platinum nanoparticles on the electrochemical parameters of OR at $\omega_0 = 1.5$

$C(\mathrm{Pt}) \cdot 10^5$ /mol L^{-1}	$\bar{I}(O_2)$ /μA	$-E(O_2)$ /mV	$\bar{I}(O_2^-)$ /μA	$-E(O_2^-)$ /mV	$\bar{I}(H_2O_2)$ /μA	$-E(H_2O_2)$ /mV
0	—	—	1.27	375	1.56	1300
1.4	—	—	1.35	306	1.32	1225
2.8	—	—	1.30	340	1.19	1220
5.6	—	—	1.06	370	1.84	1231
8.4	0.12	139	0.99	528	2.09	1240
11.2	0.98	161	0.81	541	1.70	1248

The voltammetric curve of the background solution in the absence of Pt nanoparticles (Fig. 1) has two typical broadened peaks, characteristic of the two-electron OR mechanism on the mercury electrode. The first peak with $E(O_2) = -375$ mV is related to the reaction (3), which is the reduction of molecular oxygen to H_2O_2. The second peak with $E(H_2O_2) = -1300$ mV is related to the reaction (4), which is the reduction of H_2O_2 to H_2O. The peaks on OR voltammetric curves are usually substantially broadened because of the complicated multistep process with the presence of the limiting steps. The voltammetric curves for the rapid processes have the shape of the narrow peaks; the slower the process, the stronger the peaks broadening and the lower the value of their reduction currents.

The voltammetric curve for the solution with the minimal Pt nanoparticles content (see Fig. 1, curve *1*) also consists of the two peaks, but the parameters of the peaks are substantially varied with respect to the background solution (see Fig. 1, curve *4*). The oxygen peak related to the molecular oxygen reduction ($E(O_2) = -306$ mV) is shifted to the anode region by 69 mV. The similar anode shift is also observed for the peak related to the reduction of hydrogen peroxide: $\Delta E(H_2O_2) = 75$ mV. The reduction current of oxygen $I^-(O_2)$ increases from 1.27 to 1.35 mA (see Table 1). The anode shift of the reduction peaks of O_2 and H_2O_2, as well as the increase of current $I^-(O_2)$ suggest that in solutions with the small content of Pt nanoparticles, OR proceeds in accordance with the two-electron mechanism with the lower kinetic limitations and a higher rate, than in the solutions in which Pt nanoparticles are absent.

The substantial changes are observed on the voltammetric curve (see Fig. 1, curves *2* and *3*) upon the increase in the content of Pt nanoparticles. The new peak appears at $E(O_2^-) = -139$ (curve *2*) and -161 mV (curve *3*). The main peak $E(O_2)$ broadens and shifts to the region of negative cathode potentials to -528 and -541 mV, whereas the current of oxygen reduction $I^-(O_2)$ decreases. The peak of hydrogen peroxide reduction virtually does not change its potential, whereas the current of hydrogen peroxide reduction $I^-(H_2O_2)$ increases (see Table 1).

The presence of the strong peak of H_2O_2 reduction unambigously suggests that OR follows the two-electron mechanism. The first peak of volammetric curve (for the background solution at $E(O_2) = -375$ mV) is the overall wave associated with the first step of O_2 reduction (reaction (3)). The first sub-step (reaction (3a)) with the intermediate formation of the dioxygen anion O_2^- is the rate-limiting one. The anion O_2^- stabilization was found[9] for OR in the presence of some organic substances.

The presence of weakly broadened distinct peaks in the anode region $E(O_2^-) \approx -150$ mV can be explained by the increase of the reaction (3a) rate caused by the presence of Pt nanoparticles. The increase in the rate of reaction (3a) rate results in the increase in the concentration of $HO_2^{\cdot}$ radicals and, therefore, in the increase in the rate of reaction (3b): $HO_2^{\cdot} + H^+ + e^- \longrightarrow H_2O_2$, that is reflected in the increase in the H_2O_2 reduction current.

The results of analysis of inversed voltammetry on DME of micellar solutions of Pt nanoparticles with the solubilization extent $\omega_0 = 3$ are listed in Table 2 and shown in Fig. 2. Two strong waves of OR are observed on voltammetry curves. The peaks at cathode potentials from

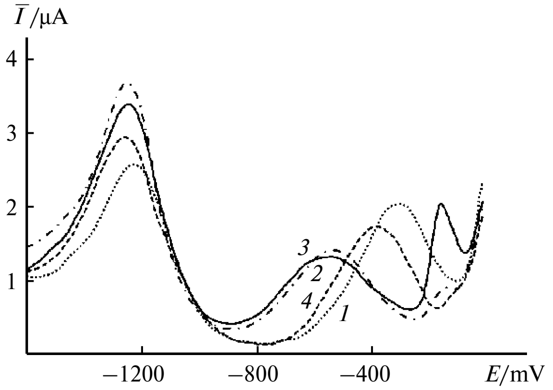

Fig. 1. The electrocheimical characteristics of OR in the presence of platinum nanoparticles at $\omega_0 = 1.5$: $C(\mathrm{Pt}) = 1.4 \cdot 10^{-5}$ (*1*), $8.4 \cdot 10^{-5}$ (*2*), $11.2 \cdot 10^{-5}$ (*3*), and 0 mol L^{-1} (*4*).

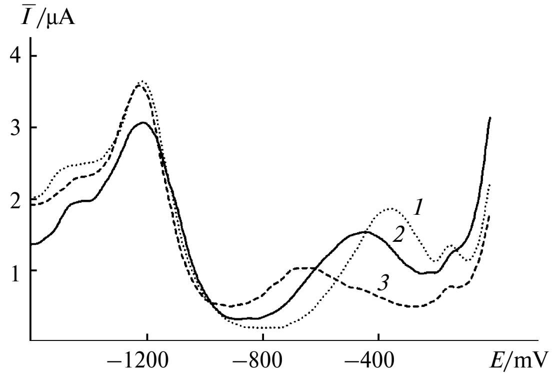

Fig. 2. The electrocheimical characteristics of OR in the presence of platinum nanoparticles at $\omega_0 = 3$: $C(\mathrm{Pt}) = 5.6 \cdot 10^{-5}$ (*1*), $16.8 \cdot 10^{-5}$ (*2*), and $28 \cdot 10^{-5}$ mol L^{-1} (*3*).

Table 2. The influence of concentration of platinum nanoparticles on the electrochemical parameters of OR at $\omega_0 = 3$

$C(\mathrm{Pt}) \cdot 10^5$ /mol L^{-1}	$\bar{I}(O_2)$ /μA	$-E(O_2)$ /mV	$\bar{I}(O_2^-)$ /μA	$-E(O_2^-)$ /mV	$\bar{I}(H_2O_2)$ /μA	$-E(H_2O_2)$ /mV
2.8	0.08	150	1.15	413	1.55	1239
5.6	0.22	145	0.97	358	1.51	1228
11.2	0.12	150	0.82	447	1.70	1246
16.8	+	150	0.80	500	1.40	1246
22.4	+	150	0.82	450	1.53	1246
28	+	150	0.55	653	1.25	1256

−1225 to −1256 mV correspond to the reduction of H_2O_2 to H_2O in accordance with the two-electron mechanism. Additional shoulder in a cathode region at $E = -1500$ mV is observed along with the main intensive peaks due to H_2O_2 reduction. The character of H_2O_2 reduction peaks remains virtually unchanged at all concentration of the Pt nanoparticles. The only exception is the peak corresponding to the sample with the maximal Pt content ($C = 2.8 \cdot 10^{-4}$ mol L^{-1}); its reduction current deacreases ($I^- = 1.25$ μA).

In the region of potentials of $E(O_2^-) = -150$ mV weak peaks are observed for all samples with $\omega_0 = 3$, but maximal reduction current is typical of the solutions with a low concentration of nanoparticles. Let us analyse the data (see Table 2 and Fig. 2), concerning the main wave of molecular dioxygen reduction in OR. With increasing concentration of Pt nanoparticles the currents of oxygen reduction $\bar{I}(O_2)$ decrease from 1.15 to 0.55 μA, the reduction potentials $E(O_2^-)$ shift to the cathode region from −413 to −653 mV, the substantial peak broadening is observed. Similar results in the frames of two-electron mechanism of OR catalysis should suggest the decrease of the process rate in the presence of Pt nanoparticles.

Characteristics of voltammetric curves as a function of the duration of contact of mercury electrode with the solution of nanoparticles were evaluated for the futher inquiry about OR mechanism in the presence of Pt nanoparticles. The voltammetric curves at $\omega_0 = 3$ with Pt concentration $C(\mathrm{Pt}) = 2.8 \cdot 10^{-4}$ mol L^{-1} at different duration of the contact with the solution are shown in Fig. 3. At $\tau = 31$ and 46 min four typical peaks (−150, −420, −660 and −1250 mV) are observed on the voltammetric curves. The increase of reduction peak $E(O_2^-) = -150$ mV suggests the catalytic action of nanoparticles on the step (3a) when the two-electron OR mechanism is operative.

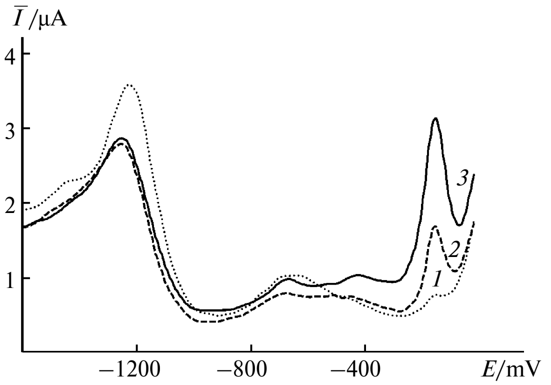

Fig. 3. The electrocheimical characteristics of OR in the presence of platinum nanoparticles at $\omega_0 = 3$ and $C(\mathrm{Pt}) = 2.8 \cdot 10^{-4}$ mol L^{-1}, obtained at the different duration of contact on the mercury electrode: $\tau = 1$ (*1*), 36 (*2*), and 46 min (3).

With the increasing duration of the contact the broadened peak of oxygen reduction (see Fig. 3, curve *3*) is divided to two components: −660 and −400 mV. The $E(O_{ads}) = -660$ mV potential is typical of the four-electron mechanism OR (steps (1) and (2)) on Pt catalysts.[9–11] The reduction potentials in the region near 400 mV were registered in our work for the electrode step (3) when OR proceeds *via* the two-electron mechanism in the absence or at a low content of Pt nanoparticles (see Tables 1 and 2).

Therefore, for $\omega_0 = 3$ at low Pt concentration the two-electron mechanism is prefered for the catalytic step (3). That is indicated by the lower overvoltage of the reduction of both O_2, and H_2O_2 and the appearance of the peak at $E(O_2^-) = -150$ mV. When the content of Pt nanoparticles increases in the solution the OR can proceed in accordance with the four-electron mechanism typical of platinum group metals. This is confirmed by both the splitting of peak of oxygen reduction into two peaks and the reduction of hydrogen peroxide reduction current $\bar{I}(H_2O_2)$ (see Figs 2 and 3).

In solutions with $\omega_0 = 1.5$ at increased Pt nanoparticles concentrations, OR, probably, can proceed in accordance with the two-electron as well as with the four-electron mechanism. This is suggested by the shift of the peaks of

Table 3. The influence of concentration of platinum nanoparticles on the electrochemical parameters of OR at $\omega_0 = 5$

$C(\mathrm{Pt}) \cdot 10^5$ /mol L^{-1}	V /mL	$\bar{I}(O_2)$ /μA	$-E(O_2)$ /mV	$\bar{I}(H_2O_2)$ /μA	$-E(H_2O_2)$ /mV	$\bar{I}(H_2O_2)'$ /μA	$-E(H_2O_2)'$ /mV
4.66	0.1	1.44	350	1.59	1225	+	1500
9.32	0.2	1.26	380	1.49	1235	+	1500
13.98	0.3	1.27	379	1.60	1235	+	1500
32.62	0.7	1.07	410	1.40	1241	+	1500

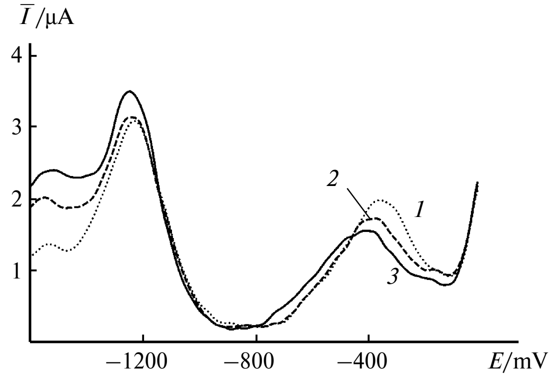

Fig. 4. The electrocheimical characteristics of OR in the presence of platinum nanoparticles at ω_0 = 5: *C*(Pt) = $4.66 \cdot 10^{-5}$ (*1*), $9.32 \cdot 10^{-5}$ (*2*), and $32.62 \cdot 10^{-5}$ mol L^{-1}(*3*).

oxygen reduction $E(O_2)$ to the cathode region and their broadening (see Table 1 and Fig. 1) observed when the concentration of Pt nanoparticles increases.

The voltammetric parameters of OR of solutions containing Pt nanoparticles at ω_0 = 5 on DME are listed at Table 3 and shown in Fig. 4. The strong peak of H_2O_2 reduction and the absence of the substantial changes in the pattern of the peak of O_2 reduction relatively to the background solution indicate that at ω_0 = 5 OR proceeds *via* the two-electron mechanism.

How can the catalytic action of Pt nanoparticles be interpreted? Let us compare the data obtained for the solution with ω_0 = 5 with the result of analysis of the background solution and the solutions with another values of ω_0. The wave parameters of H_2O_2 reduction are changed; in this case, not only anode shift of the main peak $E(H_2O_2)$ = −(1225—1241) mV relative to the background is observed, but the increase of reduction current of the cathode shoulder in the region with $E(H_2O_2{}^*)$ = −1500 mV is also registered. This is distinctly clear for the sample with the highest Pt content.

The observable splitting of the overall wave of H_2O_2 reduction into two peaks can be interpreted due to the fact, that the mechanism of H_2O_2 reduction includes two sub-steps (reactions (4a) and (4b)). The increase of the current of cathode shoulder (see Fig. 4) suggests the increase in the rate of the limiting step (4a) upon the increase in the concentration of Pt nanoparticles:

$$H_2O_2 + e^- \longrightarrow HO^{\bullet} + HO^-.$$

Such catalytic influence on H_2O_2 reduction in OR is not typical of Pt macroparticles.[9—12] The presence of peroxides results in the sharp decrease in the catalytic activity of Pt because of the formation of oxides. As indicated above, the silver is considered as the most effective catalyst of hydrogen peroxide reduction. In order to elaborate the results of catalytic action of Pt nanoparticles on OR, the influence of nanoparticles of Ag on OR was studied.

To evaluate some features of catalytic action of Ag nanoparticles on OR, the voltammetric analysis of aqueous-alcohol solutions with the solubilization extent ω_0 = 1.5 was performed. The results (Table 4, Fig. 5) allow one to conclude that the influence of Ag and Pt nanoparticle on OR is essentially different (see Figs 1 and 5). In addition, the presence of the strong peak of H_2O_2 reduction indicates that OR proceeds on DME in accordance with the two-electron mechanism.

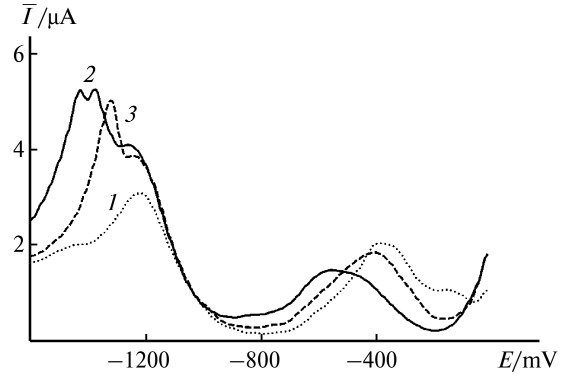

Fig. 5. The electrocheimical characteristics of OR in the presence of silver nanoparticles at ω_0 = 1.5: *C*(Ag) = $12 \cdot 10^{-4}$ (*1*), $4.8 \cdot 10^{-4}$ (*2*), and $7.2 \cdot 10^{-4}$ mol L^{-1} (*3*).

Table 4. The influence of concentration of silver nanoparticles on the electrochemical parameters of OR at ω_0 = 1.5

$C(Ag) \cdot 10^4$ /mol L^{-1}	$\bar{I}(O_2)$ /μA	$-E(O_2)$ /mV	$\bar{I}(H_2O_2)$ /μA	$-E(H_2O_2)$ /mV	$\bar{I}(H_2O_2)'$ /μA	$-E(H_2O_2)'$ /mV
1.2	1.27	362	2.12	1225	+	1500
2.4	1.45	376	2.47	1281	+	1500
4.8	1.11	553	+	1280	3.56	1423
7.2	1.44	410	+	1280	3.80	1322
8.4	1.42	428	2.54	1224	+	1500
9.6	1.68	408	2.48	1217	+	1500
10.8	1.56	415	2.33	1210	+	1500
12	1.44	415	2.48	1220	+	1500

There are notable differences in characteristics of the voltammetric curves between solutions with concentrations $C(\text{Ag}) = 4.8 \cdot 10^{-4}$ and $7.2 \cdot 10^{-4}$ mol L^{-1} (see Table 4 and Fig. 5, curves *2* and *3*) and solutions containing Ag in another concentrations. A particular evidence is the splitting of the wave of H_2O_2 reduction into two components. But, while for the majority of the samples the cathode component is a hardly perceptible shoulder, for the samples with silver concentrations $4.8 \cdot 10^{-4}$ and $7.2 \cdot 10^{-4}$ mol L^{-1} it is represented by the high values of current $\bar{I}(H_2O_2{}^*)$ and with the distinct narrow peaks. Both the broadened anode peak and the novel narrow peaks on the voltammetric curve are characterized by a lower overvoltage of reduction if the anode is estimated in relation to the background ($E = -1300$ mV), and the novel peaks – to the cathode component in another samples ($E = -1480$ mV)).

According to the two-electron mechanism the wave of H_2O_2 reduction is the superposition of two peaks associated with the rate-limiting reaction[9,10] (4a) that involves reduction of H_2O_2 molecule with the cleavage of the single oxygen—oxygen bond and the final reaction (4b) of H_2O reduction.

Accordingly, the first and the second sub-steps of H_2O_2 reduction can be descriminated as a result of selective catalytic action of Ag nanoparticles. This offers the possibility of using electrochemical data to estimate catalytic activity. The increase of reduction currents of H_2O_2 and the substantial decrease of the width of cathode peak suggest the substantial increase in the rate of the rate-limiting step (reaction (4a)), which results in the increase of the rate of the subsequent reaction (4b) of H_2O_2 reduction. It can be assumed that because of selective electrocatalytic action of Ag nanoparticles on the first sub-step of one-electron H_2O_2 decomposition *via* the two-electron mechanism of catalysis the rates of the first and the second steps of the second stage of OR are levelled off.

The results on the selective action of Ag nanoparticles help to explain the bifurcation of the wave of H_2O_2 reduction under the influence of Pt nanoparticles. They confirm the previously made assumption, that the peak with the lower value of potential can be ascribed to reaction (4a), whereas the peak with the higher value of potential is attributable to reaction (4b) for Pt nanoparticles at $\omega_0 = 5$.

At the high concentrations of low-sized fractions (2—5 nm) with $\omega_0 = 1.5$ in the presence of Pt nanoparticles the cumulative catalysis occurs. It proceeds *via* the four-electron mechanism that is typical for the bulky platinum catalysts and follows two-electron mechanism of OR not typical for Pt. Apparently, prior to the reduction step, the O_2 molecules are dissociatively adsorbed on the platinum in accordance with the four-electron mechanism,[9,10] and, besides, they favor the formation of $O_2{}^{-\bullet}$anion-radical. The formation of $O_2{}^{-\bullet}$ anion radical favors the two-electron mechanism of OR catalysis that is not typical of Pt macroparticles. When the contribution of the Pt nanoparticles fraction with the larger (up to 10—14 nm) sizes ($\omega_0 = 5$) increases, the catalytic action leads primarily to the increase in the rate of H_2O_2 electroreduction in accordance with the two-electron mechanism.

From the data described above, the catalytic action of Ag nanoparticles in OR is explained by the cleavage of the oxygen—oxygen bond in H_2O_2 molecule upon its reduction in accordance with the two-electron mechanism, whereas for catalytic Ag macroparticles the four-electron mechanism is typical.[9,10]

Catalytic action of both Pt and Ag in OR results in formation of complexes with the oxygen and the oxygen-containing intermediates caused by specific adsorption.[11,15] The selectivity of this reaction is determined by the type of the oxygen atom coordination. For the small-sized Pt nanoparticles one-site[15] coordination of oxygen molecule polarized without dissociation and the subsequent formation of the molecular anion of dioxygen on the mercury electrode may occur in accordance with the two-electron mechanism (reaction (3a)):

$$\text{Pt—O—O} + (\text{e}^-\text{—Hg}) \longrightarrow \text{Pt} + \text{O}_2{}^- + (\text{Hg}).$$

Coordination[15] of H_2O_2 molecule to two sites on the two Pt atoms in the case of larger nanoparticles ($\omega_0 = 5$) results in the cleavage of the single bond in H_2O_2 molecule and the reduction on the cathode (reaction (4a)):

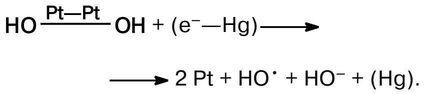

$$\text{HO}\overset{\text{Pt—Pt}}{\text{———}}\text{OH} + (\text{e}^-\text{—Hg}) \longrightarrow 2\,\text{Pt} + \text{HO}^\bullet + \text{HO}^- + (\text{Hg}).$$

Therefore, when the molecular oxygen is reduced on the electrodes even with the extremely low oxygen adsorption (such as mercury) the platinum and silver nanoparticles can form the sites that are active in catalytic reactions proceeding *via* both the two-electron and four-electron mechanisms.

The authors appreciate P. M. Zaytsev for the assistance in conducting of the electrochemical experiments.

The work was financially supported by the Russian Foundation for Basic Research (Project Nos 09-08-00547 and 09-08-00758).

References

1. N. A. Yashtulov, S. S. Gavrin, D. A. Tanasyuk, A. A. Revina, *Zh. Neorg. Khim.*, 2010, **55**, 180 [*Russ. J. Inorg. Chem.* (*Engl. Transl.*), 2010, **55**, 174].
2. N. A. Yashtulov, S. S. Gavrin, V. A. Labunov, A. A. Revina, *Nano- i mikrosistemnaya tekhnika* [*Nano and Microsystem Technics*], 2008, **8**, 20 (in Russian).
3. N. A. Yashtulov, S. S. Gavrin, *Nanoindustriya* [*Nanoindustry*], 2007, **2**, 36 (in Russian).

4. N. A. Yashtulov, A. N. Vasil´eva, E. K. Baranova, Z. M. Tomova, A. A. Revina, *Vysokie tekhnologii, fundamental´nye issledovaniya, obrazovanie* [*Hihg technologies, fundamental science, education*], Polytech. Univer. Izdat., St.-Petersburg, 2009, p. 261 (in Russian).
5. G. S. Mishra, S. Sinha, *Catal. Lett.*, 2008, **125**, 139.
6. H. Lee, S. E. Habas, G. A. Somorjai, P. Yang, *J. Am. Chem. Soc.*, 2008, **130**, 5406.
7. M. R. Tarasevich, V. A. Bogdanovskaya, B. M. Grafov, N. M. Zagudaeva, K. V. Rybalka, A. V. Kapistin, Yu. A. Kolbanovsky, *Electrokhimiya*, 2005, **41**, 840 [*Russ. J. Electrochem.* (*Engl. Transl.*), 2005, **41**, 746].
8. J. S. Wainright, R. F. Savinell, C. C. Lie, M. Litt, *Electrochim. Acta*, 2003, **48**, 2869.
9. B. B. Damaskin, O. A. Petriy, T. A. Tsyrlina, *Electrokhimiya* [*Electrochemistry*], Khimia, Moscow, 2001, 624 pp. (in Russian).
10. K. Kardesch, G. Simader, *Fuel Cells and Their Applications*, VCH, Weinheim, 1996, 375 pp.
11. F. Miomandre, S. Sadki, P. Audebert, R. Mealett-Renault, *Electrochimie*, Dunod, Paris, 2005, 360 pp.
12. M. Itagaki, H. Hasegawa, K. Watanabe, T. Hachiya, *J. Electroanal. Chem.*, 2003, **557**, 59.
13. A. A. Revina, A. N. Kezikov, E. V. Alekseev, E. B. Khailova, V. V. Volod´ko, *Nanotekhnika* [*Nanotechnics*], 2005, **4**, 105 (in Russian).
14. A. A. Revina, O. G. Larionov, L. D. Belyakova, A. V. Alekseev, *Sorbtsionnye i khromatograficheskie protsessy* [*Sorption and Chromatographic Processes*], 2004, **4**, 689 (in Russian).
15. A. Yu. Tsyvadze, *Sbornik tezisov Mezhdunarodnogo Simpoziuma po Vodorodnoi energetike* [*Abstracts of International Symposium on Hydrogen Energetics*] *(December 1—2, 2009, Moscow)*, Moscow, 2009, **74** (in Russian).

Received March 10, 2010;
in revised form July 8, 2010